

Hotspot cooling with jumping-drop vapor chambers: Supplementary material

Kris F. Wiedenheft,¹ H. Alex Guo,¹ Xiaopeng Qu,¹ Jonathan B. Boreyko,¹ Fangjie Liu,¹
Kungang Zhang,¹ Feras Eid,² Arnab Choudhury,² Zhihua Li,² and Chuan-Hua Chen^{1,*}

¹Department of Mechanical Engineering and Materials Science, Duke University, Durham, NC 27708, USA

²Intel Corporation, Chandler, AZ 85226, USA

(Dated: February 10, 2017)

S1. EXPERIMENTAL METHODS

The evaporator plate (Alloy 101, 390 W/m-K) has a cross-sectional area of 76.2 mm×76.2 mm and an initial height of 7.4 mm. At the center of the copper evaporator, a pillared wick with an area of 61.0 mm×61.0 mm and a height of 1.0 mm is created, after the four surrounding edges are cut down to flush with the bottom of the wick in preparation for gasket sealing. The squarely arranged pillars are machined using a custom-made saw blade (Malco HSS Saw, 0.004 in thickness, 1 in diameter with 98 teeth), giving rise to a nominal cross-sectional area of 0.1 mm×0.1 mm and a center-to-center separation of 0.2 mm. The 1.0 mm height is achieved by consecutive cutting operations due to the depth limitation of the saw blade. The machined wick is rendered superhydrophilic by thermal oxidization in atmospheric air, during which the entire evaporator is placed on a hotplate (Fisher Sci. 11-300-49SHP) set to 300 °C for a typical duration of 30 min. On the backside of the evaporator plate, a trench is formed by milling out the center region with an area of 42.1 mm×42.1 mm and a depth of 5.2 mm (Fig. S1). Accordingly, the center of the evaporator has a solid layer with a thickness of only 1.2 mm, excluding the wick structure described above.

For thermal characterization, a small resistive heater with an area of $A = 2.5 \text{ mm} \times 5.1 \text{ mm}$ (Am. Tech. Ceramics LR12010T0050JBK) is soldered onto the back of the trenched evaporator to provide a localized heat load. The resistive heating is controlled by a DC power supply (BK Precision 1623A). The top of the evaporator (with the soldered heater) is protected by a thermal foam to minimize heat loss. The condenser is cooled by a recirculating chiller (Thermo Fisher Sci. Accel-250-LC) using two 3.8 mm-diameter thru-holes in the condenser that are soldered to pipes with an outer diameter (OD) of 6.4 mm. The charging and evacuation ports are built into the condenser and soldered to 3.2 mm-OD pipes. Other components for charging the working fluid and evacuating noncondensable gases are detailed in Boreyko and Chen [*Int. J. Heat Mass Transfer*, vol. 61, pp. 409-418 (2013)]. The temperature of the condenser is probed at its center with a thermistor (Omega 44131), which is embedded in a 2.6 mm-diameter hole

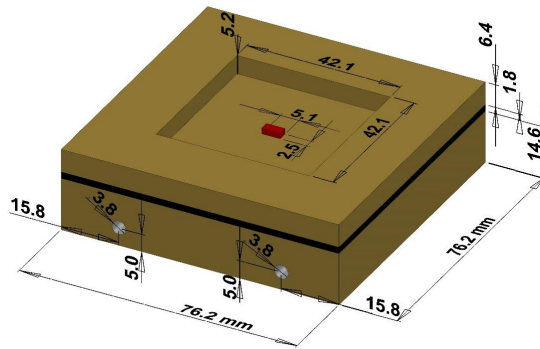


FIG. S1: The geometry of the vapor chamber with all the dimensions in millimeters. The solid enclosure is exactly reproduced while excluding the thermistor hole in the condenser, the charging and evacuation ports, and the screw holes used for compression sealing. The black layer represents the (compressed) vacuum gasket.

*Electronic address: chuanhua.chen@duke.edu

drilled with its axis parallel to and 3.6 mm below the superhydrophobic surface. Because of the thin evaporator, a thermal probe hole on the evaporator side is not possible. Instead, a small thermocouple with a bead diameter of $75\ \mu\text{m}$ (Omega Chal-003) is embedded underneath the resistive heater while the heater is soldered onto the evaporator (using Chip Quik SMD4300SNL10 solder paste). The copper evaporator is heated up to facilitate the soldering, typically at $300\ ^\circ\text{C}$ for 20 min. Care is taken to center the thermocouple bead under the resistive heater and to minimize the solder footprint to roughly match the heater area. The resulting heat flux q is nominally the input power divided by the cross-sectional area of the heater. Additional care is taken during soldering to pull the exposed portion of the two thermocouple lead-wires away from the copper plate, so as to avoid unintended electrical contact.

S2. HEAT SPREADING MODEL

Given the localized heat flux, a heat spreading factor Γ is needed to convert the $\Delta T(q)$ measurements into effective thermal conductivities k_O , as in Eq. (1). The Γ factor is obtained by numerical simulation in Fig. S2, in which the *overall* chamber (including the jumping-drop section) is modeled as an isotropic solid material with a uniform effective thermal conductivity k_O . The heat produced by the resistive heater is modeled as a localized heat flux that is uniformly distributed across the heater area. The cooling pipes in the condenser assume a constant wall temperature, and the rest of the chamber surface is assumed adiabatic. Under these boundary conditions, Γ is purely a geometrical factor, e.g. $\Gamma=0.198$ for the geometry in Fig. S2.

Two assumptions of the numerical model deserve some discussion: (i) Isothermal boundary condition is imposed on the walls of the cooling pipes carrying the circulation of refrigerated liquid. Although a convective boundary condition is more precise, a constant wall temperature is an excellent approximation because the heat source and both temperature probes are far away from the cooling pipes. For the extraction of Γ , only the temperature difference between the two probes matters in Eq. (1). In Table S1, the calculated spreading factor Γ is nearly independent of the heat transfer coefficient h of the cooling pipes, although h is varied over a broad range between 10 and $10^6\ \text{W/m}^2\cdot\text{K}$. This range encompasses the estimated coefficient of $5 \times 10^4\ \text{W/m}^2\cdot\text{K}$ based on the recirculating flow rate and inner pipe diameter. Further, all the Γ values in Table S1 are essentially equivalent to the value reported in the main paper, $\Gamma=0.198$, which is based on constant wall temperature. (ii) The overall vapor chamber assumes a uniform effective thermal conductivity k_O . An isotropic k_O is assumed to facilitate comparison with other heat spreaders, e.g. a pure copper spreader or a different vapor chamber as in the main text. In reality, the thermal conductivity of the jumping section is typically different from that of the copper enclosure, so a more elaborate model should account for the disparate thermal conductivities. However, there is a practical difficulty in the context of the jumping-drop vapor chamber with anisotropic thermal properties: the out-of-plane thermal conductivity (k_z) related to the jumping return is different from the in-plane thermal conductivity (k_{xy}) related to the wicking return. Additional work is needed to establish the relationship between the effective conductivities in different directions before a more accurate model can be developed.

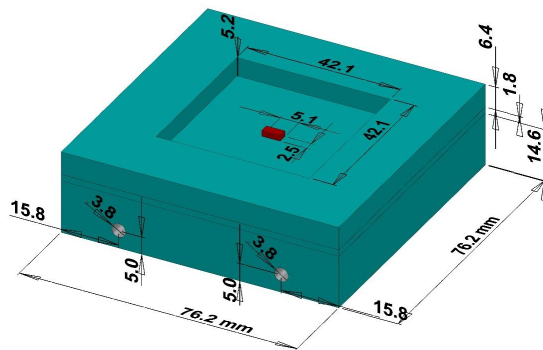


FIG. S2: Heat spreading factor is extracted from the computation of heat conduction through a solid block with a uniform thermal conductivity k_O . The solid block adopts the same dimensions as the overall vapor chamber in Fig. S1. The jumping section is replaced by a solid layer with the same thermal conductivity k_O .

TABLE S1: The spreading factor Γ is a weak function of the convection coefficient h .

wall condition	h [W/m ² ·K]	Γ [-]
convective	10	0.198213
	10 ³	0.198213
	5 × 10 ⁴	0.198223
	10 ⁶	0.198238
isothermal	∞	0.198241